JOURNAL OF AGRICULTURAL AND FOOD CHEMISTRY

Chemical Modification of Wheat Protein-Based Natural Polymers: Cross-Linking Effect on Mechanical Properties and Phase Structures

XIAOQING ZHANG,* PAM HOOBIN, IKO BURGAR, AND MY DIEU DO

CSIRO Manufacturing & Materials Technology, Private Bag 33, Clayton South MDC, Clayton South, VIC 3169, Australia

Chemical modification of wheat protein-based natural polymer materials was conducted using glyoxal as cross-linker, and the cross-linking effect was studied on mechanical properties under different humidity conditions, the molecular motions of each component, and the phase structures/components of the whole materials. The cross-linking significantly enhanced the mechanical strength of wheat gluten (WG) materials under RH = 50%. The elongation of materials was also increased, which was in contrast to many cross-linked protein systems. The reaction mainly occurred in proteins and starch components, resulting in the formation of a stable cross-linked network with restricted molecular motions and modified motional dynamics. Although the plasticizer glycerol could also take part in the reaction with glyoxal or other components in WG especially when the glyoxal content was higher, the amount of glycerol involved in such reactions was very little. Glycerol was predominantly hydrogen-bonded with the network. The lipid component did not seem to take part in the cross-linking reaction; its mobility was promoted while its interaction with the protein−starch network was weakened after cross-linking. The formation of the cross-linked network did not enhance the hydrophobicity of the materials; the materials still adsorbed a high level of moisture under high humidity conditions (ca. RH = 85%) with no improvement in mechanical strength. In addition, further increasing the amount of glyoxal did not generate an additional strength improvement even at RH = 50%, possibly because the enhanced mobility of lipid promoted the component to be phase-separated from the WG system. To improve the water-resistant properties, the hydrophobicity of the protein macromolecules requires enhancement by other chemical modifications.

KEYWORDS: Wheat proteins; cross-linking; mechanical performance; molecular motions; solid-state NMR

INTRODUCTION

Wheat gluten (WG) is a promising renewable and biodegradable natural polymer with high potential for technical application due to its unique intrinsic properties, low price, and large-scale availability with consistent quality. WG protein-based edible films have been prepared via solution casting, and the film formation performance has been studied comprehensively with regard to plasticizing effect, film formation solutions, thermal effect, pH effect, and conformation changes of WG during the film formation process (*1*−*15*). However, films prepared from the proteins usually show low mechanical strength, weak water resistance, and poor water vapor barrier properties. Aldehyde cross-linkers have been widely used in many protein-based materials such as wheat gluten (*16*, *17*), soy proteins (*18*−*20*), collagen (*21*), corn zein (*22*), whey proteins (*23*), cottonseed proteins (*24*, *25*), and even wool fibers (*26*, *27*) to promote the cross-linked network formed with the protein aggregated structures and to enhance the mechanical properties. Other cross-linkers such as carbodiimides (*28*, *29*), epoxy compounds (*30*, *31*) and genipin (*31*) have also been studied for protein systems. Aldehyde-based cross-linkers (formaldehyde, glyoxal, and glutaraldehyde) have shown the most effective cross-linking effect on the structure and performance of proteins.

Developing WG-based natural polymer materials for the packaging industry is a great challenge for materials scientists as sufficient mechanical strength and water-resistant properties are usually required in the application. Thermal processing technologies such as compression molding or extrusion would not only produce WG-based materials more efficiently and avoid the solvent usage as in solution casting, but also promote the thermal cross-linking of WG macromolecules and improve the mechanical strength of the materials (*5*, *6*, *32*−*36*). Introduction of chemical cross-linkers into the WG systems would further enhance the formation of covalent bonds within the aggregated network because thermal processing conditions are also favor-

* Corresponding author. Telephone: +63 95452653. Fax: +613 95441128. E-mail: Xiaoqing.Zhang@csiro.au.

10.1021/jf061597q CCC: $33.50
Published on Web 11/18/2006

able for formation of chemical cross-linking; thus, mechanical strength and barrier properties of the WG materials would be further improved. Although many chemical processes that happen in the solution casting could be present in the thermal processing, less research has been reported on the cross-linking effect on structure and mechanical performance of thermally processed WG materials.

In this article, glyoxal was taken as a typical aldehyde cross-linker and used in WG materials with water and glycerol as plasticizers. Glyoxal has been used in the paper packaging industry to replace formaldehyde as it is less volatile and the price is also low. High alkaline conditions have been reported as being favorable for the formation of WG film and glyoxal cross-linking, but such conditions are undesirable for edible packaging (*37*−*39*). Our recent study on thermally processed WG materials (*40*, *41*) indicated that alkaline conditions significantly impacted the strength of WG films with water only as a plasticizer, while the effect was not significant when glycerol was used. A cross-linked network was formed within the whole WG materials during thermal processing under either acidic or alkaline conditions (*40*). Therefore, an acidic condition (pH = 4) was chosen to process the cross-linked materials. It is desirable that the cross-linked network formed under these conditions should be stable under acidic hydrolysis. The cross-linking effect on the mechanical performance of WG materials under standard humidity (RH ≈ 50%) and high humidity (RH ≈ 85%) was examined. Dynamic mechanical analysis (DMA) and solid-state NMR spectroscopy were conducted under the standard humidity condition to study the cross-linking effect on phase compositions, molecular motions of each individual component, and intermolecular interactions among different components in the WG materials. The cross-linking chemistry of the system is also discussed.

MATERIALS AND METHODS

Materials. WG vital, supplied by Manildra Group Australia, contained about 80% proteins, 15% residual starch, 4% lipid, and around 1% fibers and other impurities on dry basis. The moisture content was 12%. Sheet samples of the WG system were prepared using glycerol (15 wt %) and water (15 wt %) as plasticizers. The pH of the plasticizers was adjusted to 4.0 using acetic acid. A small amount of Na_2SO_3 (0.3% to WG) was added into all systems to dissociate the disulfide bonding within the protein chains to achieve efficient mixing between proteins and plasticizers. Glyoxal (gx, 40% in water), obtained from Sigma-Aldrich, was mixed into the plasticizers with varying amounts (0.7, 1.4, and 2.1 wt %). Each WG-gx sample with a designed formulation was mixed with a high-speed mixer operated at a speed of 3000 rpm for 1 min, left overnight, and then compression-molded at an optimum temperature of 130 °C for 5 min using a heating press with a pressure of 12 ton. The sample size was 145 mm × 145 mm with a thickness of 1.0 mm ± 0.1 mm. DMA and solid-state NMR experiments were conducted on samples after the conditioning at RH = 50%, while tensile strength was tested after conditioning the samples for one week at room temperature under both humidity conditions (RH = 50% or RH = 85%). The loss of plasticizers after drying the sample at 105 °C for 24 h was 9.2−9.5% or 20.3−20.7% for samples after conditioning under a standard humidity (RH = 50%) or a high humidity (RH = 85%) condition at room temperature for a week, respectively.

Instrumentation. Tensile strength of the samples was measured on an INSTRON 5566P at room temperature with crosshead speed of 50 mm/min. Dog-bond specimens with an effective length of 30 mm and width of 6 mm were obtained by cutting the compression-molded sheet samples, and the mechanical strength data for each sample were obtained from an average of testing seven such specimens.

DMA experiments were conducted on a Perkin-Elmer PYRIS Diamond DMA in dual cantilevers bending mode at a frequency of 1 Hz. The temperature range was set at −100 to 150 °C with a heating rate of 2 °C/min. The storage modulus (E'), the loss modulus (E''), and tan δ (E''/E') were recorded as a function of temperature throughout the experiment.

Broad line pulse solid-state ^{1}H NMR was carried out on a Bruker Minispec PC 120 spectrometer at 20 MHz. The 90° pulse was 4.5 μs with repetition of 2 s. The free induction decay (FID) signal of each sample was obtained by a solid-echo pulse sequence (*42*) and a Carr−Purcel−Meiboom−Gill (CPMG: 90°x-(t_1-180°y-t_1-echo)n) pulse sequence (*42*), respectively, at 40 °C. The 90−180° pulse spacing (t_1) in the CPMG sequence was 50 μs, n was varied, and eight scans were used for each measurement. The whole FID of each sample was a combination of the data observed from solid-echo (time range of 0−0.15 ms) and from CPMG (time range of 0.4−8.0 ms) pulse sequences, and then the FID data were best-fitted by multidecay functions using the IGOR program from Wave Metrics, Inc.

High-resolution solid-state NMR experiments were conducted at room temperature using a Varian Unity plus spectrometer at resonance frequencies of 75 MHz for ^{13}C and 300 MHz for ^{1}H. ^{13}C NMR spectra were observed using either cross-polarization, magic angle spinning, and high power dipolar decoupling (CP/MAS/DD) technique, or a single 90° pulse excitation (SPE) method with high power decoupling. The 90° pulse was 4.5 μs for H-1 and C-13 (rf strength for spin-locking was 56 kHz), while the spinning rate of MAS was set at a value in the range of 6 to 7 kHz. A contact time of 1.0 ms was used for measuring CP/MAS spectra, while the repetition time was 2 s. The chemical shift of ^{13}C spectra was determined by taking the carbonyl carbon of solid glycine (176.03 ppm) as an external reference standard. ^{1}H MAS NMR spectra were obtained with the same MAS rates, and TMS was used as an external chemical shift reference. ^{1}H spin−spin (T_2) relaxation times under high-resolution conditions (MAS) were measured either through the decay of ^{13}C magnetization prepared by CP with varied CP delay times as reported previously (*36*, *40*, *43*), or through the decay of ^{1}H intensities in MAS spectra observed by the CPMG (t_1 of 40 μs) pulse sequence with a repetition time of 2 s and a 90° pulse length of 2.5 μs. The ^{13}C spin−lattice relaxation times in rotating frame ($T_{1\rho}$) were measured from the decay of magnetization during ^{13}C spin-locking pulse after preparation of the magnetization through CP (*43*). ^{1}H and ^{13}C solution NMR spectra were measured using the same spectrometer with a solution probe head.

RESULTS AND DISCUSSION

Mechanical Properties and T_g Behavior of the Materials. Due to the hydrophilic nature of WG components, the materials are normally very sensitive to moisture and the mechanical properties strongly depend on the moisture content in the materials and the humidity condition in the storage environment. Mechanical properties of WG-gx materials were measured under two different humidity conditions, and the results are listed in **Table 1**. Under standard humidity condition (RH = 50%), the tensile strength of the materials increased significantly after reaction with gx. The maximum strength improvement was reached when 1.4% of gx was used, but a further increase of the gx content to 2.1% resulted in a strength reduction. The modulus displayed a similar trend as the tensile strength. This strength performance is consistent with those obtained for solution cast films; however, the strength improvement was not accompanied by a decrease in elongation, as found in most cross-linked protein systems. In contrast, the elongation of the materials even increased to some extent at RH = 50% when gx was used, although the increase was not significant when using 1.4% of gx at which the maximum strength enhancement was reached. After the samples were conditioned under high humidity conditions (RH = 85%), the tensile strength decreased remarkably due to a high moisture content (∼20%) in the materials. The strength improvement was not significant, and the cross-linking effect was observed in the increase of modulus and decrease of elongation for the materials. The results

Table 1. Mechanical Properties of the WG-gx Materials

samples	glyoxal (%)	tensile strength (Mpa)		elongation @ break (%)		Young's modulus (Mpa)	
		RH = 52%	RH = 85%	RH = 52%	RH = 85%	RH = 52%	RH = 85%
WG-gx0	0	5.8	3.0	106.4	238.9	65.4	43.4
WG-gx1	0.7	10.5	3.2	149.6	215.4	98.2	45.5
WG-gx2	1.4	14.0	3.2	112.1	175.5	121.3	50.2
WG-gx3	2.0	11.5	2.9	143.1	168.6	92.2	65.1

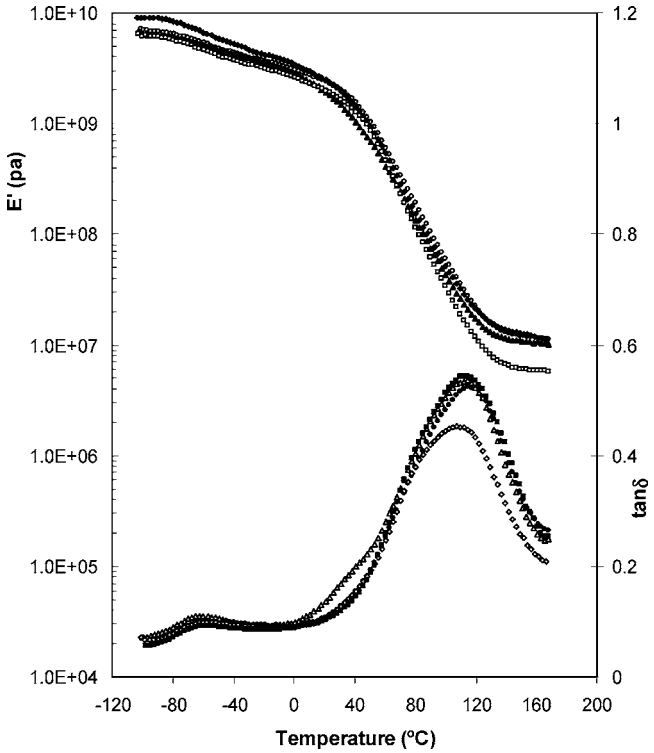

Figure 1. Storage modulus (E') and tan δ of the WG-gx materials obtained from DMA. E' and tan δ of WG-gx0 (○, ●), WG-gx1 (▲, △), WG-gx2% (◆, ◇), and WG-gx3 (□, ■).

indicated that cross-linking WG with gx during thermal processing under acidic conditions did result in a significant tensile strength improvement under standard humidity conditions. As the moisture content in all of these samples was quite similar, the strength improvement was not derived from the enhancement of hydrophobicity of the materials but from the additional cross-linking effect in the aggregated network. These materials, however, still easily absorbed additional moisture under a high humidity condition, and the high moisture content was the main factor for the tensile strength. The cross-linking effect played a minor role then, but it could still be observed in the decrease in elongation and increase of modulus for the WG-gx materials.

The DMA data of the WG-gx materials are shown in **Figure 1**. In general, the behavior of these WG-gx materials was similar, but the cross-linking effect was indeed observed. The highest E' value at temperatures below the T_g transition was detected for WG-gx2 (using 1.4% of gx). As the temperature increased, all samples experienced a significant E' decrease due to T_g transitions of the materials. Some key DMA data of the WG-gx systems are listed in **Table 2**. The E' onset corresponding to the T_g transition occurred at around 33 °C for WG-gx0, WG-gx2, and WG-gx3, while that of WG-gx1 shifted to 13 °C. A significant tan $\delta-\alpha$ peak was detected for each of the samples due to the T_g transition. The tan $\delta-\alpha$ maximum was the lowest in WG-gx2, while those of the other three samples were similar, indicating the highest motional restriction of the aggregated structure formed in WG-gx2 corresponding to the cross-linking. A tan $\delta-\alpha$ shoulder was observed for WG-gx1 around 15 °C, being consistent with the E' decrease onset occurring at a lower temperature. The minor onset of E' decreases in conjunction with a tan $\delta-\beta$ peak at around −60 °C obtained for all WG-gx samples were due to β-transitions of the plasticized systems as described previously (*35*, *36*). These weak tan $\delta-\beta$ peaks remained at the same temperature range, but the intensity decreased from 0.11 (WG-gx0) to 0.09 (WG-gx3), indicating that the motional dynamics of the β-transition was also restricted by the cross-linking.

Although the cross-linking only modified the T_g of the WG materials slightly, it did cause a significant strength improvement under RH = 50%. The maximum strength improvement was 140% achieved when 1.4% of gx was used. Such cross-linking also generated an increase in elongation. However, the covalent bonds formed during cross-linking were still hydrophilic, and the materials could easily absorb additional moisture under high humidity condition (ca. RH = 85%); such cross-linking did not result in strength improvement for the materials when the moisture content was high.

Cross-Linking Effect on the Molecular Motions and Phase Compositions. The molecular motions and phase compositions of plasticized WG materials have been studied by solid-state NMR and reported recently (*35*, *40*). In a complex polymer system such as plasticized multicomponent WG, various phases with a wide distribution of molecular mobility coexisted even at temperatures above the T_g. The molecular mobility and phase compositions of the plasticized WG materials had a direct relationship with their mechanical performance. The same methodology was applied to study the cross-linking effect on the WG-gx materials in this article.

^{1}H spin−spin relaxation (T_2) was detected via measuring FID signals for WG-gx materials as it is sensitive to the mobility of polymers at molecular levels (*42*). As reported previously (*40*), FID signals were obtained by a combination of the signals detected via solid-echo (sensitive to rigid components) and CPMG (sensitive to mobile components) and analyzed by best fitting using a model function containing a Gaussian decay with a short T_2 (T_{2S}) and two exponential decays with longer T_2 values (T_{2M} and T_{2L}). The three components could be referred to as rigid, intermediate, and mobile phases. The ^{1}H T_2 data (including T_{2S}, T_{2M}, and T_{2L} values and the proportion of each component as phase composition) of WG-gx systems are shown in **Figure 2A**,**B**. As the amount of gx increased, the T_2 values of T_{2S} and T_{2M} slightly decreased while those of T_{2L} increased. Meanwhile, as the gx content increased in the materials, the proportion of T_{2S} (rigid phase) increased while that of T_{2L} phase decreased. The proportion of T_{2S} increased from 42 ^{1}H % (WG-gx0) to 50 ^{1}H % (WG-gx3), while the T_{2L} proportion was reduced from 23 ^{1}H % (WG-gx0) to 15 ^{1}H % (WG-gx3). Interestingly, the

Table 2. Key DMA Data of the WG-gx Materials

samples	tan δ–β (°C)	tan δ–β maximum	T_g from E' onset (°C)	tan δ–α (°C)	tan δ–α maximum
WG-gx0	–57	0.11	34	115	0.522
WG-gx1	–60	0.11	13	114	0.536
WG-gx2	–60	0.10	33	108	0.454
WG-gx3	–60	0.09	32	112	0.543

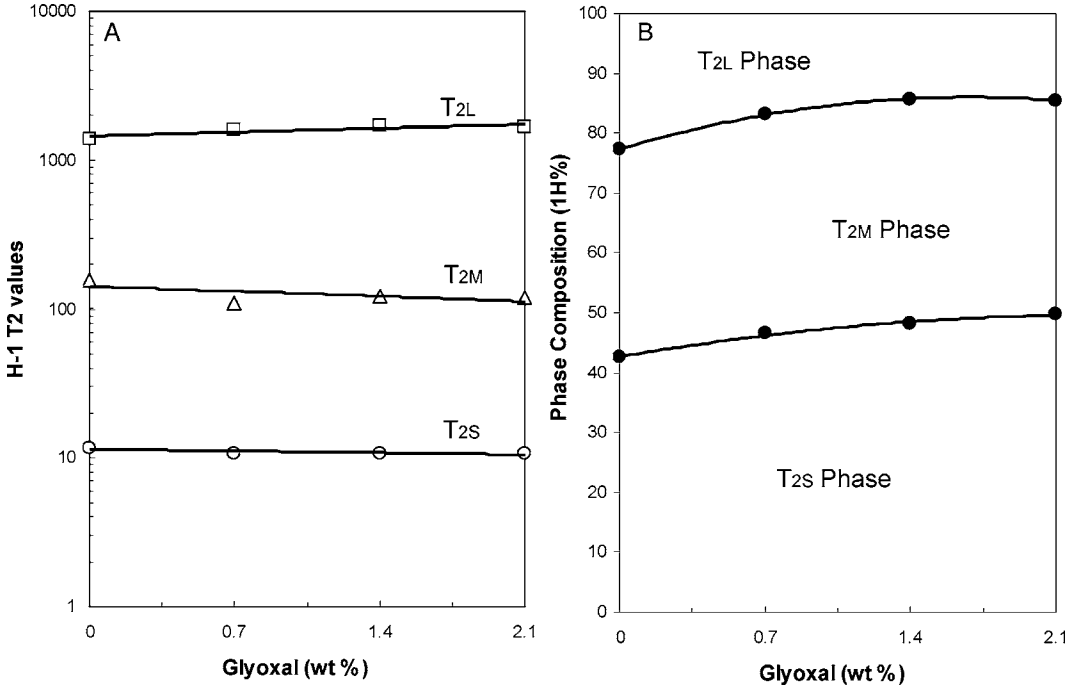

Figure 2. (**A**) ^{1}H T_{2S}, T_{2M}, and T_{2L} values (μs). (**B**) Proportion of each component (phase composition) (●) of WG-gx materials.

proportion of T_{2M} remained at 35 ^{1}H %. The results indicate that the cross-linking reactions caused a development of the rigidity of the T_{2S} and T_{2M} phases, and molecular motions in these phases were restricted. Some parts of the molecules in the mobile phase (possibly the plasticized proteins) also took part in the cross-linking reactions. However, such cross-linking also weakened the interactions between mobile phase and other components and caused the mobile components to become further mobile. This could be one reason that the strength of the materials did not further improve with additional gx content (ca. 2.1%) in the materials.

High-resolution solid-state NMR provides an advanced technique to explore the behavior of each individual component in a complicated system with good resolution and selectivity. The CP/MAS method was sensitive to the rigid phase of polymer components as the transition of proton magnetization to ^{13}C resonances requires strong dipolar interactions in the systems that normally have relatively static motions of polymer chains. On the other hand, only very mobile components can be obtained in ^{1}H MAS NMR spectra as the MAS condition (MAS speed of 6−8 kHz) is usually not sufficient to average out the strong proton dipolar interactions in the rigid phase and these resonances would appear as a very broad peak contributing to the baseline. **Figure 3** shows the ^{13}C CP/MAS and ^{1}H MAS spectra of WG-gx materials. Mainly proteins (173, 132, 54, and 30−25 ppm) and starch (103, 83, and 74 ppm) were observed in the ^{13}C CP/MAS spectra, while glycerol signals, as sharp peaks, were also observed at 74 and 64 ppm. Mobile components obtained in the ^{1}H MAS spectra are due to water and glycerol (4.5−3.7 ppm) in conjunction with lipid (0.9, 1.3, 2.0, 2.7, and

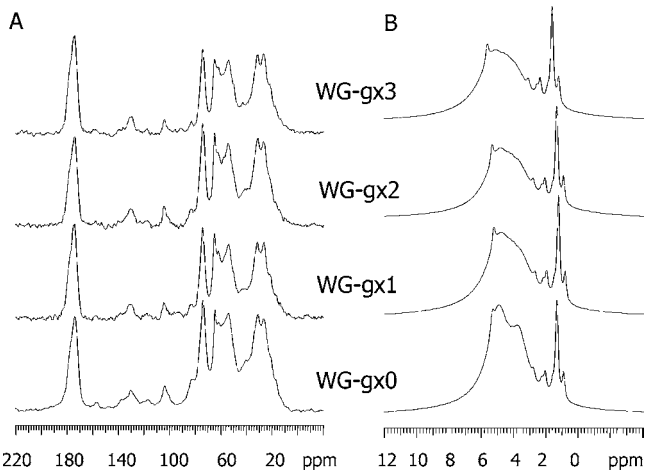

Figure 3. ^{13}C CP/MAS (**A**) and ^{1}H MAS (**B**) NMR spectra of the WG-gx materials.

5.3 ppm) (*40*, *44*). Examination of the relaxation behavior through these individual resonances (components) via the high-resolution NMR spectra can show the change of molecular motions of these components after cross-linking.

The ^{1}H T_2 values of WG-gx materials measured via ^{13}C CP/MAS NMR with varied CP delay times are shown in **Table 3**. As found for plasticized WG materials (*36*), the resonances of proteins and starch decayed very fast as the CP delay time increased, following a single Gaussian decay model. However, the T_2 values observed at 174 and 54 ppm (proteins) and 103 ppm (starch) decreased when gx was present, indicating the

Table 3. ^{1}H T_2 Values (μs) of the WG-gx Samples Obtained via ^{13}C CP/MAS Spectra

samples	174 ppm	102 ppm	74 ppm	64 ppm	54 ppm	25–30 ppm
WG-gx0	13.7	16.3	15.2/52% 114/48%	14.8/26% 107/74%	13.0	13.2
WG-gx1	12.0	14.6	16.2/69% 113/31%	15.1/44% 97/56%	11.8	12.7
WG-gx2	11.3	10.2	15.5/71% 109/29%	14.6/43% 105/57%	11.9	12.3
WG-gx3	11.3	10.1	15.8/75% 97/25%	15.2/58% 107/42%	11.4	11.9

Table 4. ^{1}H T_2 Values (ms) of the WG-gx Samples Obtained via ^{1}H MAS Spectra

samples	4.5–3.7 ppm	2.1 ppm	1.3 ppm	0.9 ppm
WG-gx0	0.69	2.1	18.9	4.65
WG-gx1	0.55	3.1	23.2	4.69
WG-gx2	0.57	4.5	25.6	10.3
WG-gx3	0.53	4.1	23.1	8.55

cross-linking did enhance the aggregation structure of proteins and starch in the rigid phase. The two T_2 components of glycerol at 74 and 64 ppm were also observed in WG-gx systems following a model function of one Gaussian and one exponential decay (*36*). The shorter T_2 values of the glycerol resonances did not change greatly but the proportion increased when the gx content increased, while the values of the longer T_2 components became shorter when gx was used. It seems that the motional state of glycerol was also restricted to some extent in the rigid and intermediate phases, possibly due to the development of rigidity of proteins and starch network in conjunction with an enhancement of intermolecular interactions between glycerol and WG macromolecules.

The cross-linking effect on the mobile phase lipid and water/glycerol could be examined by measuring the ^{1}H T_2 values via ^{1}H MAS spectra with CPMG pulse sequence. The data are summarized in **Table 4**. In general, the T_2 of water or water/glycerol (at 4.5−3.7 ppm) decreased slightly with increasing gx content, and the values were still much lower than those of lipid (at 2.1, 1.3, and 0.9 ppm) in all systems. The lipid displayed different behavior for each resonance, but the T_2 values observed from most of the resonances/groups increased when gx was used. This indicated that the mobility of lipid was promoted after cross-linking proteins and starch with gx and contributed to the enhanced mobility of T_{2L} phases as shown in **Figure 2**. The enhanced mobility of lipid also suggested that its weaker interaction with other WG components and most likely the lipid did not take part in the cross-linking reactions.

Cross-Linking Reactions in the System. The reactions between gx and proteins in solution were studied in a series of reports (*17*, *25*). The aldehyde groups in gx would react with the amine groups of lysine or the phenolic structures of tyrosine to form acid hydrolysis-resistant covalent bonds for protein cross-linking. Reactions with arginine would produce reversible products under alkaline conditions. Other primary amines and thiol groups in the proteins could also react with gx to form chemical linkages between different protein chains. In addition, the hydroxyl groups of starch could also take part in the reactions with gx to form acetal bonds. Under a thermal processing condition used in this study (130 °C), these reactions and further thermal condensation of the products formed in these reactions would then form stable chemical bonds to build up a cross-linked network within the proteins and starch phase. However, many of these functional groups formed in the reactions could still be sensitive to water and tend to adsorb moisture under high humidity conditions.

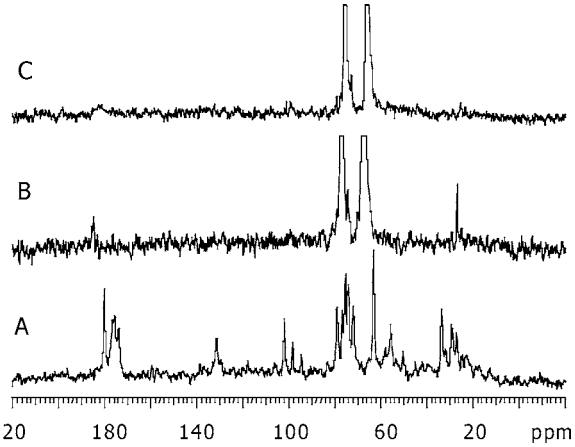

Figure 4. ^{13}C solution NMR spectra of the water phases after sonication of (**A**) WG powders, (**B**) WG-gx0, and (**C**) WG-gx2.

It was suggested previously that glycerol could take part in the thermal cross-linking reactions with wheat proteins under heating conditions that stabilized the systems and contributed to the strength of the materials (*32*, *45*). In plasticized WG-gx systems, gx could also react with the hydroxyl groups of glycerol (functionality of 3) in conjunction with starch or proteins and generate a polymer network containing glycerol structures. To study whether such reactions occurred in the process, the retention of glycerol was measured as described below.

WG-gx samples were soaked in distilled water (5% solid) under sonication. The samples were then washed by distilled water and dried at room temperature to a constant moisture content of 4 to 5%. We avoided further drying the samples because it might have added another factor for change of the WG structures. The glycerol content in the water after the sonication was measured by ^{1}H solution NMR spectra using TMS in a constant concentration as internal reference. In all WG-gx (WG-gx0 to -gx3) samples, the amount of glycerol in water after sonication for 1 h was quite close (within 1 to 2%) to the amount added to the systems during thermal processing. This indicated that, even if glycerol took part in the cross-linking reaction, the amount would be very small. Most of the glycerol molecules were still hydrogen-bonded to the WG without chemical bonding.

Figure 4 shows the ^{13}C solution NMR spectra of the water phases after sonication of WG powder, WG-gx0, and WG-gx2 samples for 5 h. Around 35% of WG was dissolved in water after such sonication, and the dissolved portion was mainly assigned to starch and soluble proteins. After thermal processing, whether with or without gx, mainly the signals of glycerol (74 and 64 ppm) and acetic acid (183 and 27 ppm) were detected as extracted into the water phase. In WG-gx2 after cross-linking with gx, it was surprising to notice that the intensity of acetic acid became lower or the line width became broad in the water phase.

Possible reactions between glycerol and gx in the systems were also studied. **Figure 5A** shows the ^{13}C solution NMR spectrum of gx solution (40%), where gx remained in the hydrated state and formed oligomers with ^{13}C resonances located in a range of 90−110 ppm. Glycerol and gx were mixed according to the ratio in WG-gx2, and the pH was also adjusted to 4.0 by acetic acid. After the clear glycerol−gx solution was heated to 130 °C for 10 min, the ^{13}C solution NMR spectrum

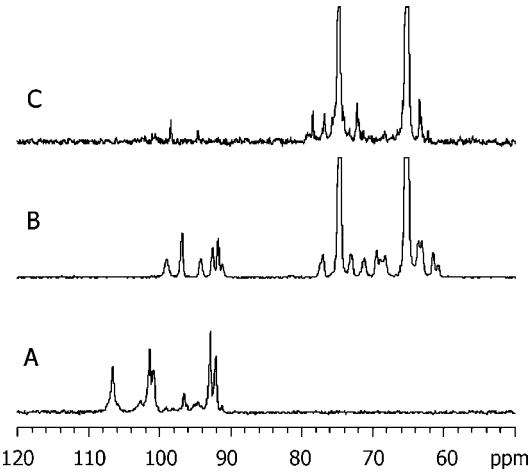

Figure 5. ^{13}C solution NMR spectra of (**A**) glyoxal solution (40%), (**B**) products of the glycerol–glyoxal reaction, and (**C**) the water phase after sonication of WG-gx3.

was detected as shown in **Figure 5B**. Various new resonances were observed around 60−80 ppm and 90−100 ppm, indicating that gx could react with glycerol under the material processing condition for WG-gx samples. The ^{13}C NMR spectrum of the water phase after sonication of WG-gx3 (the gx content was 2.1%, **Figure 5C**) does show groups of similar resonances in the same range, indicating such reactions did occur in the WG-gx system especially when the gx content was higher. Although some glycerol involved in the cross-reactions with gx and WG might be retained in the WG cross-linked network, it did not generate any positive impact on the mechanical performance of the materials as no additional strength improvement was obtained in WG-gx3 sample.

The CP/MAS and SPE ^{13}C NMR spectra of WG-gx0 and WG-gx2 after removal of plasticizers are shown in **Figure 6**. All glycerol signals disappeared in both spectra, and what remained in the CP/MAS spectra were proteins (174, 132, 54, and 30−25 ppm) and starch (103, 83, and 74 ppm). Mobile lipid was the main component detected in the SPE spectrum (at 179, 130, 30−23, and 15 ppm) in conjunction with a minor amount of mobile proteins (174, 60−45, and 30−15 ppm) and starch (74 ppm). The intensities at 61 and 52 ppm in the SPE spectrum indicated the presence of proline and glutamine, respectively, being consistent with previous reports that proline and glutamine were the easiest segments in wheat proteins to be plasticized or hydrated (*14*, *32*, *44*). The removal of plasticizers made it possible to study the cross-linking effect on the WG components with no influence from plasticization.

^{13}C spin−lattice relaxation times in the rotating frame (^{13}C $T_{1\rho}$) provide many advantages to study motions for glassy polymers where ^{1}H T_2 all appear around 10 μs (*46*−*49*). It is sensitive to the motions at a frequency range of 10−100 kHz, which are the characteristic frequencies of cooperative motions of polymer chains. The relaxation times would not be averaged out by spin diffusion effect as happens in ^{1}H $T_{1\rho}$ relaxations; thus, the motional information of each specific site can be retained especially under MAS conditions. Two components (spin−lattice and spin−spin relaxations) are normally involved in ^{13}C $T_{1\rho}$ relaxations, where the spin−spin process is a function of the dipolar field strength with no relation to molecular motions. It has been well-established that the spin−lattice relaxation is predominant in amorphous polymers while the spin−spin process is significant for crystalline polymers. For amorphous WG-gx materials, the ^{13}C $T_{1\rho}$ (listed in **Table 5**) should reflect the motional information of each group and component in the materials and approach a minimum corresponding to the T_g transition.

As the water content was only 4 to 5% in all these samples, the T_g transition of these samples would occur at a temperature much higher than room temperature. Thus, the ^{13}C $T_{1\rho}$ values of WG-gx samples should all be located at the left side of the ^{13}C $T_{1\rho}$ minimum, where the longer relaxation times indicate the more restrictions present to the molecular motions. A single ^{13}C $T_{1\rho}$ component was obtained as an average relaxation process of many resonances overlapped at 174, 74, and 54 ppm for proteins and starch, but the resonances at 30−25 ppm did appear as two components. No attempt was made to analyze the relaxation dynamics in detail; only the data change after cross-linking was examined here. Note that the cross-linking with gx did cause an increase in ^{13}C $T_{1\rho}$ values for all resonances, and the longest values were observed for WG-gx2, which displayed the strongest strength improvement. Due to the broad line width of each component and overlapping of resonances in the materials, it is difficult to specify which resonance/group was directly involved in the reactions, but the C═O groups at 174 ppm should not have taken part in the reactions. In fact, the ^{13}C $T_{1\rho}$ value of the C═O groups in **Table 5** also increased after the cross-linking, indicating that the restriction of molecular motions occurred in the whole aggregated network. The results were consistent with the decrease of T_{2S} and T_{2M} data shown in **Figure 2**, but the ^{13}C $T_{1\rho}$ result provided evidence that the increase of rigidity of materials occurred in the proteins and starch component of the materials.

The cross-linking effect on the lipid component in WG was further examined after removal of the plasticizers. **Figure 7** shows the ^{1}H MAS spectra of WG-gx0 and WG-gx2 when plasticizers were removed. Only lipid signals (*44*) were obtained in both cases, while the broad peak of other rigid components appeared as baseline. The ^{1}H T_2 values of lipid in these samples were obtained by CPMG pulse sequence via ^{1}H MAS spectra as listed in **Table 6**. As compared to the data shown in **Table 4**, the ^{1}H T_2 values of all lipid resonances became longer. The methylene resonances (1.3 ppm) only increased slightly, while the $-CH_2-COO-$ (2.1 ppm), and $-CH_3$ (0.9 ppm) resonances rose significantly as compared to the systems with plasticizers. Such mobility enhancement for lipid suggested that the plasticizer played a key role as a compatibilizer between lipid and protein−starch in the materials and the lipid might interact with proteins and starch via the plasticizer. Note from **Table 6** that the T_2 values of lipid further increased when gx was used in the system, indicating that the cross-linking reactions further enhanced the mobility of lipid, and this mainly contributed to the enhanced mobility of T_{2L} phases as shown in **Figure 2**. Such a mobility enhancement of lipid would reduce the intermolecular interactions between lipid and other components in the materials and thus promote the lipid molecules to be phase-separated from the system, which played a negative role in the materials strength as seen by the mechanical performance of the WG-gx3 sample.

Conclusions. The cross-linking reaction with glyoxal significantly enhanced the mechanical strength of the WG materials under RH = 50% in conjunction with an increase in elongation. Such reactions mainly occurred in proteins and starch components, resulting in formation of a stable cross-linked network with more restricted molecular motions and modified motional dynamics. The plasticizer glycerol could also take part in the reactions with glyoxal and other components in WG especially when the gx content was higher. However, the amount of glycerol involved in such reactions was very little, and the molecules predominantly hydrogen-bonded with the network.

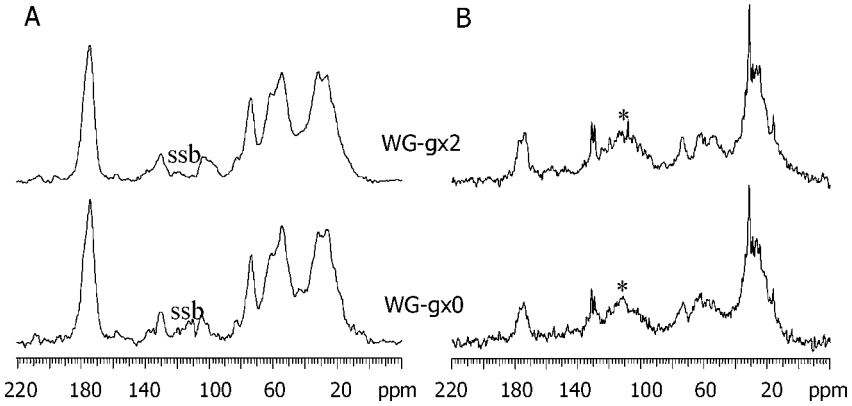

Figure 6. ^{13}C CP/MAS (**A**) and SPE (**B**) NMR spectra of the WG-gx materials after removing glycerol plasticizer. ssb = spinning sidebands, * = background signals of the spinner.

Table 5. ^{13}C $T_{1\rho}$ Values (ms) of the WG-gx Samples after Removing Glycerol Plasticizer

samples	174 ppm	74 ppm	54 ppm	30 ppm
WG-gx0	22.9	2.4	2.6	0.93/61% 14.1/39%
WG-gx1	23.7	2.8	2.9	0.89/67% 17.8/33%
WG-gx2	26.8	3.4	3.5	2.0/69% 24.4/31%
WG-gx3	22.3	2.6	2.7	1.1/69% 18.1/31%

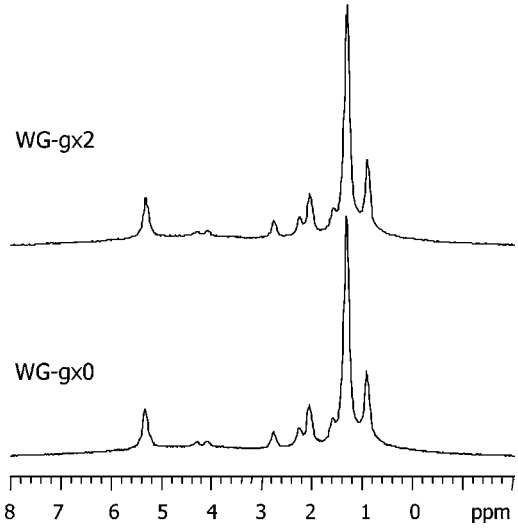

Figure 7. ^{1}H MAS NMR spectra of the WG-gx0 and WG-gx2 samples after removing glycerol plasticizer.

Table 6. ^{1}H T_2 Values (ms) of the WG-gx Samples Obtained via ^{1}H MAS Spectra after Removing Glycerol Plasticizer

samples	5.3 ppm	2.7 ppm	2.1 ppm	1.3 ppm	0.9 ppm
WG-gx0	21.1	9.0	16.5	24.6	21.1
WG-gx1	25.6	14.7	18.9	26.3	24.5
WG-gx2	26.3	15.5	18.8	26.7	23.0
WG-gx3	26.9	16.7	20.9	27.2	24.8

The lipid component did not react with glyoxal while its mobility was promoted, and its interaction with the network was weakened after the cross-linking. The formation of the cross-linked network did not enhance the hydrophobicity of the materials; the materials still adsorbed a high level of moisture under high humidity conditions (ca. RH = 85%), and no improvement of mechanical strength was obtained. Additionally, further increasing the amount of glyoxal did not show an additional strength improvement even at RH = 50%, possibly because the mobility enhancement of lipid caused the lipid component to be phase-separated from the system, which had a negative effect on the strength of the materials. To improve the water-resistant properties of the materials, other chemical modifications are required to enhance the hydrophobicity of wheat protein macromolecules.

LITERATURE CITED

(1) Ali, Y.; Ghorpade, V. M.; Hanna, M. A. Properties of thermally-treated wheat gluten films. *Ind. Crops Prod.* **1997**, *6*, 177−184.

(2) Gontard, N.; Ring, S. Edible wheat gluten film: Influence of water content on glass transition temperature. *J. Agric. Food Chem.* **1996**, *44*, 3474−3478.

(3) Pouplin, M.; Redl, A.; Gontard, N. Glass transition of wheat gluten plasticized with water, glycerol, or sorbitol. *J. Agric. Food Chem.* **1999**, *47*, 538−543.

(4) Irissin-Mangata, J.; Bauduin, G.; Boutevin, B.; Gontard, N. New plasticizers for wheat gluten films. *Eur. Polym. J.* **2001**, *37*, 1533−1541.

(5) Pommet, M.; Redl, A.; Morel, M. H.; Guilbert, S. Study of wheat gluten plasticized with fatty acids. *Polymer* **2003**, *44*, 115−122.

(6) Redl, A.; Morel, M.; Bonicel, J.; Vergnes, B. Guibert, S. Extrusion of wheat gluten plasticized with glycerol: Influence of process conditions on flow behavior, rheological properties, and molecular size distribution. *Cereal Chem.* **1999**, *76*, 361−370.

(7) Redl, A.; Morel, M.; Bonicel, J.; Guibert, S.; Vergnes, B. Rheological properties of gluten plasticized with glycerol: Dependence on temperature, glycerol content and mixing conditions. *Rheol. Acta* **1999**, *38*, 311−320.

(8) Zhang, X.; Burgar, I.; Do, M.; Lourbakos, E.; Beh, H. Wheat protein and its polymer blends studied by solid-state high-resolution NMR spectroscopy. *Polym. Prepr. (Am. Chem. Soc., Div. Polym. Chem.)* **2003**, *44*, 402−403.

(9) Pommet, M.; Redl, A.; Guibert, S.; Morel, M.-M. Intrinsic influence of various plasticizers on functional properties and reactivity of wheat gluten thermoplastic materials. *J. Cereal Sci.* **2005**, *42*, 81−91.

(10) Apichartsrangkoon, A.; Ledward, D.; Bell, A.; Brennan, J. Physicochemical properties of high pressure treated wheat gluten. *Food Chem.* **1998**, *63*, 215−220.

(11) Graaf, L. Denaturation of proteins from a non-food perspective. *J. Biotechnol.* **2000**, *79*, 299−306.

(12) Elizalde, B. E.; Pilosof, A. M. R. Kinetics of physico-chemical changes in wheat gluten in the vicinity of the glass transition temperature. *J. Food Eng.* **1999**, *42*, 97−102.

(13) Hargreaves, J.; Popineau, Y.; Le Meste, M.; Hemminga, M. A. Molecular flexibility in wheat gluten proteins submitted to heating. *FEBS Lett.* **1995**, *372*, 103−107.
(14) Micard, V.; Guilbert, S. Thermal behaviour of native and hydrophobized wheat gluten, gliadin and glutenin-rich fractions by modulated DSC. *Int. J. Biol. Macromol.* **2000**, *27*, 229−236.
(15) Lens, J.-P.; de Graaf, L. A.; Stevels, W. M.; Dietz, C. H. J. T.; Verhelst, K. C. S.; Vereijken, J. M.; Kolster, P. Influence of processing and storage conditions on the mechanical and barrier properties of films cast from aqueous wheat gluten dispersions. *Ind. Crops Prod.* **2003**, *17*, 119−130.
(16) Micard, V.; Belamri, R.; Morel, M.-H.; Guilbert, S. G. Properties of chemically and physically treated wheat gluten films. *J. Agric. Food Chem.* **2000**, *48*, 2948−2953.
(17) Hernández-Muñoz, P.; Villalobos, R.; Chiralt, A. Effect of cross-linking using aldehydes on properties of glutenin-rich films. *Food Hydrocolloids* **2004**, *18*, 403−411.
(18) Ghorpade, V. M.; Li, H.; Gennadios, A.; Hanna, M. A. Chemically modified soy protein films. *Trans. ASAE* **1995**, *38*, 1805−1808.
(19) Park, S. K.; Bae, D. H.; Rhee, K. C. Soy protein biopolymers cross-linked with glutaraldehyle. *J. Am. Oil Chem. Soc.* **2000**, *77*, 879−883.
(20) Rhim, J. W.; Gennadios, A.; Handa, A.; Weller, C. L.; Hanna, M. A. Solubility, tensile, and color properties of modified soy protein isolate films. *J. Agric. Food Chem.* **2000**, *48*, 4937−4941.
(21) Lieberman, E. R.; Guibert, S. G. Gas permeation of collagen films as affected by crosslinkage, moisture and plasticizer content. *J. Polym. Sci., Polym. Symp.* **1973**, *41*, 33−43.
(22) Parris, N.; Coffin, D. R. Composition factors affecting the water vapor permeability and tensile properties of hydrophilic zein films. *J. Agric. Food Chem.* **1997**, *45*, 1596−1599.
(23) Galiett, G.; di Gioia, L.; Guilbert, S.; Cuq, B. Mechanical and thermomechanical properties of films based on whey proteins as affected by plasticizer and crosslinking agents. *J. Dairy Sci.* **1998**, *81*, 3123−3130.
(24) Marquie, C.; Aymard, C.; Cuq, J. L.; Guilbert, S. Biodegradable packaging made from cottonseed flour: Formation and improvement by chemical treatments with gossypol, formaldehyde, and glutaraldehyde. *J. Agric. Food Chem.* **1995**, *43*, 2762−2767.
(25) Marquie, C. Chemical reactions in cottonseed protein cross-linking by formaldehyde, glutaraldehyde, and glyoxal for the formation of protein films with enhanced mechanical properties. *J. Agric. Food Chem.* **2001**, *49*, 4676−4681.
(26) Happich, W. F.; Windus, W.; Naghski, J. Stabilization of wool by glutaraldehyde. *Text. Res. J.* **1965**, *35*, 850−852.
(27) Di Monica, G.; Marzona, M. Crosslinking of wool keratin by bifunctional dialdehydes. *Text. Res. J.* **1971**, *41*, 701−705.
(28) Tropini, V.; Lens, J.-P.; Mulder, W. J.; Silvestre, F. Wheat gluten films cross-linked with 1-ethyl-3-(3-dimethylaminopropyl) carbodiimide and *N*-hydroxysuccinimide. *Ind. Crops Prod.* **2003**, *20*, 281−289.
(29) Kuijpers, A. J.; Engbers, G. H. M.; Feijen, J.; de Smedt, S. C.; Meyvis, T. K. L.; Demeester, J.; Krijgsveld, J.; Zaat, S. A. J.; Dankert, J. Characterization of the network structure carbodiimide cross-linked gelatin gels. *Macromolecules* **1999**, *32*, 3325−3333.
(30) Van, Wachem, P. B.; Zeeman, R.; Dijkstra, P. J.; Feijen, J.; Hendriks, M.; Cahalan, P. T.; van Luyn, M. J.A. Characterization and biocompatibility of epoxy-crosslinked dermal sheep collagens. *J. Biomed. Mater. Res.* **1999**, *47*, 270−277.
(31) Sung, H.-W.; Huang, D.-M.; Chang, W.-H.; Huang, R.-N.; Hsu, J.-C. Evaluation of gelatin hydrogel crosslinked with various crosslinking agents as bioadhesives: In vitro study. *J. Biomed. Mater. Res.* **1999**, *46*, 520−530.
(32) Micard, V.; Morel, M.-H.; Bonicel, J.; Guilbert, S. Thermal properties of raw and processed wheat gluten in relation with protein aggregation. *Polymer* **2001**, *42*, 477−485.
(33) Gallstedt, M.; Mattozzi, A.; Johansson, E.; Hedenqvist, M. S. Transport and tensile properties of compression-molded wheat gluten films. *Biomacromolecules* **2004**, *5*, 2020−2028.
(34) Zhang, X.; Do, M.; Lourbakos, E. Strength enhancement of wheat protein based biodegradable polymer materials. *Polym. Prepr. (Am. Chem. Soc., Div. Polym. Chem.)* **2005**, *46*, 321−322.
(35) Zhang, X.; Burgar, I.; Lourbakos, E.; Beh, H. The mechanical property and phase structures of wheat proteins/polyvinyl alcohol blends studied by high-resolution solid-state NMR. *Polymer* **2004**, *45*, 3305−3312.
(36) Zhang, X.; Burgar, I.; Do, M.; Lourbakos, E. Intermolecular interactions and phase structures of plasticized wheat proteins materials. *Biomacromolecules* **2005**, *6*, 1661−1671.
(37) Kato, A.; Tanaka, A.; Lee, Y.; Matsudomi, N.; Kobayashi, K. Effects of deamidation with chymotrypsin at pH 10 on the functional properties of proteins. *J. Agric. Food Chem.* **1987**, *35*, 285−288.
(38) Gennadios, A; Brandenburg, A. H.; Weller, C. L.; Testin, R. F. Effect of pH on properties of wheat gluten and soy protein isolate films. *J. Agric. Food Chem.* **1993**, *41*, 1835−1839.
(39) Kayserilioglu, B. S.; Stevels, W. M.; Mulder, W. J.; Akkas, N. Mechanical and biochemical characterization of wheat gluten films as a function of pH and co-solvent. *Starch* **2001**, *53*, 381−386.
(40) Zhang, X.; Do, M.; Hoobin, P.; Burgar, I. The phase composition and molecular motions of plasticized wheat gluten-based biodegradable polymer materials studied by solid-state NMR spectroscopy. *Polymer* **2006**, *47*, 5888.
(41) Zhang, X.; Hoobin, P.; Burgar, I.; Do, M. The pH effect on the mechanical performance and phase mobility of thermally processed wheat gluten-based natural polymer materials. *Biomacromolecules* **2006**, in press.
(42) McBrierty, V.; Packer, K. *Nuclear Magnetic Resonance in Solid Polymers*; Cambridge University Press: Cambridge, U.K., 1993.
(43) Alexlson, D. E.; Russell, K. Characterization of polymers by means of ^{13}C NMR spectroscopy: (a) Morphology by solid-state NMR (b) End-group studies. *Prog. Polym. Sci.* **1985**, *11*, 221−282.
(44) Friedman, M. Chemistry, biochemistry, nutrition, and microbiology of lysinoalanine, lanthionine, and histidinoalanine in food and other proteins. *J. Agric. Food Chem.* **1999**, *47*, 1295−1317.
(45) Calucci, L.; Forte, C.; Galleschi, L.; Geppi, M.; Ghiringhelli, S. ^{13}C and ^{1}H solid state NMR investigation of hydration effects on gluten dynamics. *Int. J. Biol. Macromol.* **2003**, *32*, 179−189.
(46) Schaefer, J.; Stejskal, E. O.; Buchdahl, R. Magic-angle ^{13}C NMR analysis of motion in solid glassy polymers. *Macromolecules* **1977**, *10*, 384−405.
(47) Schaefer, J.; Sefcik, M. D.; Stejskal, E. O.; McKay, R. A. Carbon-13 $T_{1\rho}$ experiments on solid polymers having tightly spin-coupled protons. *Macromolecules* **1984**, *17*, 1118−1124.
(48) Simmons, A.; Natansohn, A. Carbon-13 CP/MAS NMR chemical shift and molecular dynamics study of charge-transfer interactions in blends of poly(2-[(3,5-dinitrobenzoyl)oxy]ethyl methacrylate) with poly[(*N*-ethylcarbazol-3-yl)methyl methacrylate or acrylate]. *Macromolecules* **1992**, *25*, 3881−3889.
(49) Jack, K. S.; Whittaker, A. K. Molecular motion in miscible polymer blends. 1. Motion in blends of PEO and PVPh studied by solid-state ^{13}C $T_{1\rho}$ measurements. *Macromolecules* **1997**, *30*, 3560−3568.

Received for review June 7, 2006. Revised manuscript received September 21, 2006. Accepted October 10, 2006.

JF061597Q